

## SCIENCE OF TSUNAMI HAZARDS

Journal of Tsunami Society International

Volume 38

Number 2

2019

### IDENTIFICATION OF TSUNAMIGENIC EARTHQUAKE ZONES IN OCEANIC RIDGES AND TRENCHES

O.S. Hammed<sup>1</sup>, T.A. Adagunodo<sup>2</sup>, M.O. Awoyemi<sup>3</sup>, A.B. Arogundade<sup>3</sup>, O.D. Ajama<sup>3</sup>, F.O. Sapele<sup>1</sup>, M.R. Usikalu<sup>2</sup>, A.M. Olanrewaju<sup>4</sup>, S.A. Akinwumi<sup>2</sup>, E.I. Ogunwale<sup>2</sup>

<sup>1</sup> Department of Physics, Federal University, Oye-Ekiti, Nigeria.

<sup>2</sup> Department of Physics, Covenant University, Ota, Nigeria.

<sup>3</sup> Department of Physics, Obafemi Awolowo University, Ile-Ife, Nigeria.

<sup>4</sup> Department of Mathematics, Covenant University, Ota, Nigeria

Email addresses: [olaide.hammed@fuoye.edu.ng](mailto:olaide.hammed@fuoye.edu.ng); [theophilus.adagunodo@covenantuniversity.edu.ng](mailto:theophilus.adagunodo@covenantuniversity.edu.ng);  
[ajobay@oauife.edu.ng](mailto:ajobay@oauife.edu.ng)

#### ABSTRACT

Tsunamigenic earthquakes have been known for their near and far field catastrophic impacts on coastal areas near oceanic ridges and trenches, as well as near tectonic faults in closed and semi-enclosed seas. Not all regions of oceanic ridges and trenches are tsunamigenic earthquake zones, but knowledge of the weighted sum of released earthquake energy and of the Gutenberg-Richter relation of the 'a' and 'b' parameters are needed to better identify them as to their potential for tsunami generation. The present analysis was undertaken in order to better identify tsunamigenic zones near oceanic ridges and trenches in the Mid-Atlantic, in the Pacific, in Chile, in Japan, near the Aleutians and along the Peru-Chile trench. The weighted sum of earthquake energy released and of the Gutenberg-Richter relation parameters were evaluated to identify tsunamigenic earthquake zones along these locations. The present analysis of the Gutenberg-Richter relation of the 'a' and 'b' parameters indicates that tsunamigenic earthquakes do not occur frequently along the Aleutian Trench, although the historic record supports that destructive tsunamis have occurred along this region in the past. Of the oceanic ridges, the results of the present analysis indicate that the Mid-Atlantic Ridge is the most active tsunamigenic zone, while of all the oceanic trenches, the Japan Trench is the most active.

**Keywords:** *b-value, a-value, tsunamigenic, oceanic ridges, oceanic trenches*

## 1. INTRODUCTION

Large earthquakes of relatively shallow focal depth near oceanic ridges and trenches can generate destructive tsunamis. (Adagunodo and Sunmonu, 2015). The term tsunamigenic earthquake was introduced by [Kanamori](#) (Kanamori, 1972) for events associated with such destructive waves. Some of the better known historical tsunamigenic earthquakes are the [1994 Java earthquake](#) (Bryant, 2008), the [1996 Chimbote earthquake](#) (Polet, 2000), the [2006 Pangandaran earthquake and tsunami](#) (Ammon et al., 2006), and the 1570 to 2015 tsunamis/earthquakes in Chile (Adagunodo et al., 2018a). Tsunamigenic earthquakes occur frequently but extremely destructive events for certain areas may occur as long apart as every 800 years (Pararas-Carayannis, 2011; Adagunodo et al. 2018a). These kinds of earthquakes are those that usually exceed 7.5 Richter magnitudes.

Most disastrous tsunamis are generated by shallow, great earthquakes near tectonic subduction zones (Figure 1). More than 80% of the world's tsunamis occur along subduction zones in the perimeter in the Pacific, often referred to as the “Ring of Fire”. Tsunamis were particularly catastrophic impacts in certain areas in the world. For example, the tsunami generated by the 27 March 1964 Alaska earthquake, damaged heavily communities along the Gulf of Alaska, Kodiak Island and Prince William Sound area as well as in the Bay of Valdez - killing 107 people (Pararas-Carayannis, 1967). On 17 July 1998, four villages on Papua - New Guinea’s north coast were almost entirely swept away by tsunami waves. The 1896 Sanriku (Japan) earthquake generated a 35 meter high tsunami that washed away 10,000 homes and killed 26,000 people. The 1964 Alaska earthquake created a 7 meter high tsunami that struck a power station, plunging in darkness the city of Hilo on the island of Hawaii. In addition, Adagunodo et al. (2018a) reported that tsunamis and earthquakes within recorded history have rendered about 1.8 million people homeless.

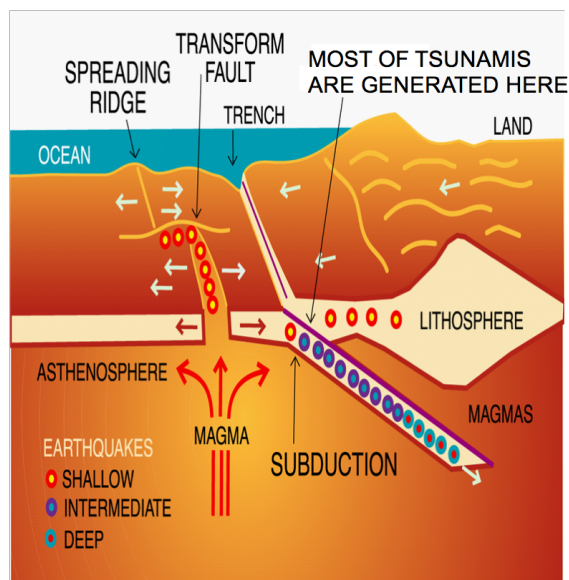


Figure 1: Generation of tsunamigenic earthquakes at subduction zone.

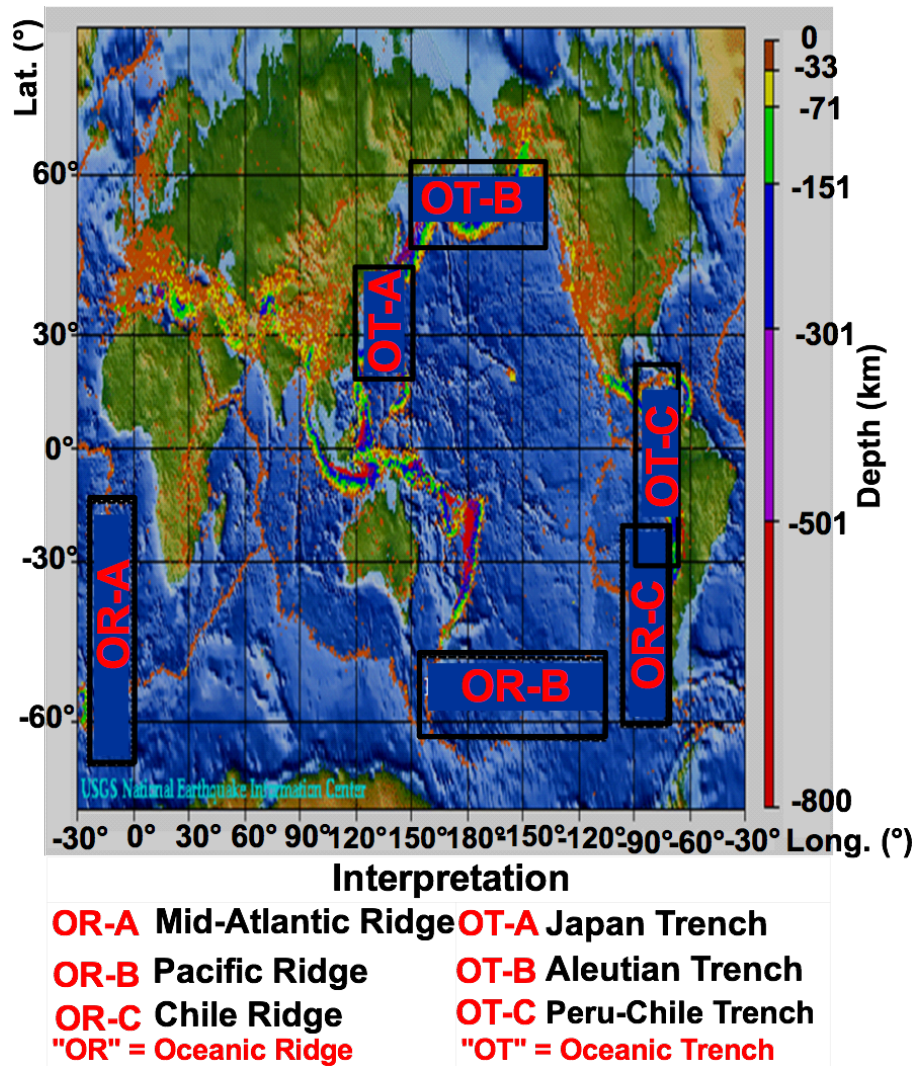
A standard method in providing early warnings for tsunami is based on data that identifies an earthquake as potentially tsunamigenic and is able to predict the possible size and destructiveness of the waves (Tsuboi, 2000). In the present study, the weighted sum of earthquake energy released and the frequency-magnitude distribution of the earthquakes were used to identify the tsunamigenic earthquake zones in three oceanic ridges (Chile Ridge, Mid-Atlantic Ridge and Pacific Ridge) and three trenches (Aleutian Trench, Japan Trench and Peru-Chile Trench) respectively. Identification of earthquake occurrences in such regions facilitates the issuance of tsunami warnings (Adagunodo and Sunmonu, 2015). Analyses of seismically active zones have been reported by some researchers (Hammed et al., 2013; Awoyera et al., 2016; Awoyemi et al., 2017; Awoyera et al., 2017; Adagunodo et al., 2018b; and Hammed et al., 2018).

## **2. DATA ACQUISITION, DESCRIPTION AND METHOD**

The data used for this study were obtained from the earthquake catalogue of the Advance National Seismic System (ANSS) hosted by the Northern California Earthquake Data Centre U.S.A in a readable format. The data comprised of earthquakes occurring along the mid-ocean ridges and trenches with magnitudes of  $2.0 \leq M \leq 9.0$  from January 1, 1978 to December 31, 2017 (40-year data period). The data for each earthquake gave the date and time of occurrence, the latitude and longitude of the epicenter, the depth, the magnitude designation, and source codes and event identification. Using “Compicat” software - an earthquake catalog processing software - the data were sorted out, filtered and analyzed in order to remove errors due to data duplication and mixing.

The oceanic ridges that were studied are shown on the seismicity map in Figure 2, specifically: a) The Chile Ridge from latitude  $48^{\circ}$  to  $36^{\circ}$  S and longitude  $110^{\circ}$  to  $75^{\circ}$  W; b) The Mid Atlantic Ridge from latitude  $50^{\circ}$  S to  $20^{\circ}$  N and longitude  $45^{\circ}$  to  $10^{\circ}$  W; and c) The Pacific Ridge from latitude  $68^{\circ}$  to  $58^{\circ}$  S and longitude  $120^{\circ}$  to  $18^{\circ}$  W.

The oceanic trenches that were studied are also shown in Figure 2. Specifically examined were a) the Aleutian Trench from latitude  $51^{\circ}$  to  $53^{\circ}$  N and longitude  $160^{\circ}$  to  $176^{\circ}$  W.; b) The Japan Trench from latitude  $40^{\circ}$  to  $53^{\circ}$  N and longitude  $148^{\circ}$  to  $165^{\circ}$  E; and c) The Peru - Chile Trench from latitude  $15^{\circ}$  S to  $30^{\circ}$  N and longitude  $75^{\circ}$  to  $64^{\circ}$  E. The parameters that were evaluated were the weighted sum of earthquake energy released and the frequency-magnitude distribution of the earthquakes.



(Source: National Earthquake Information Center (NEIC), US Geological Service)

Figure 2: Map of the global seismicity (1975 – 2010) color-coded by depth

## 2.1 Method

### 2.1.1 Evaluation of Weighted Sum of Earthquake Energy Released

In order to study the seismic pattern or hazard of a region, there is a need to investigate the earthquake energy released in the earthquake prone regions to mitigate the future occurrence of earthquakes (Amiri et al., 2008; Ghosh, 2007). The earthquake energy released in oceanic ridges and trenches were plotted against the coordinates of epicenters of the earthquakes in order to understand the seismic activity of the regions (Figures 3 and 4).

### 2.1.2 Evaluation of Frequency-Magnitude Distribution (FMD) of the Earthquakes

The Frequency-Magnitude Distribution (FMD) - also known as the Gutenberg-Richter relation proposed by Charles Francis Richter and Beno Gutenberg (Richter and Gutenberg, 1944) - is commonly used in the modeling of earthquake hazard, mostly related to the earthquake precursors and probabilistic seismic hazard assessments (Nuannin, 2006; Damanik *et al.* 2010). The FMD describes the number of earthquakes occurring in a given region as a function of their magnitude  $M$  as:

$$\text{Log } N = a - bM \quad (1)$$

where  $N$  is the cumulative number of earthquakes with magnitudes equal to or greater than  $M$ , and “ $a$ ” and “ $b$ ” are real constants with values which vary in space and time. The parameter “ $a$ ” characterizes the general level of seismicity in a given area during the study period i.e. the higher the  $a$ -value, the higher the seismicity. The parameter “ $b$ ” commonly called the  $b$ -value has been widely used in the study of seismicity, tectonics, seismic risk estimation and earthquakes prediction. The  $b$ -value indicates the tectonic character of a region and assumed to depend on the accumulated stress in that region (Nuannin, 2006). Schorlemmer *et al.* (2004) described  $b$ -value as a stress meter, depending inversely on the differential stress.

For the present work, the FMD of the earthquakes along oceanic ridges and trenches were evaluated by plotting the logarithm of the cumulative number of the earthquakes as a function of their magnitudes. These plots were then fitted with straight lines that best fit the plots (Adagunodo *et al.* 2018b). The straight lines represent the Gutenberg – Richter equation as shown in Equation 1. The overall “ $a$ ” and “ $b$ ” values of earthquakes in each study region were obtained as an intercept and a slope of the line of best fit, respectively.

## 3.0 RESULTS AND DISCUSSION

### 3.1 Analysis of Weighted sum of Earthquake Energy along Oceanic Ridges

The distribution of weighted sum of earthquake energy released in the Mid Atlantic Ridge as shown in Figure 3a revealed that the earthquake energy released in the ridge is predominantly concentrated in both the southeastern and northeastern part of the ridge. However, the large earthquake energy is prevalent in the northeastern part of the ridge as shown in Figures 3b and 3c. These figures obviously revealed the image of earthquake energy distribution along the epicenter coordinates. The earthquake energy is sparsely concentrated in the southwestern region of the ridge. The extremely large energy in the eastern part of the ridge is an indication that the region is prone to continuous accumulation of oceanic lithospheric plate stress which can generate large earthquakes. A large earthquake within the oceanic ridge can generate a tsunami. The cluster of large earthquake energy in the northeastern part of the ridge is an indication that the region is an earthquake zone that has the potential of generating tsunamis. In the Pacific Ridge, the spatial distribution of earthquake energy released along the ridge is shown in Figure 3d. The latitudinal and longitudinal coordinates of the energy distribution were

also investigated (Figures 3e and f). The weighted sum of earthquake energy is predominantly distributed towards the northern part of the ridge and sparsely distributed towards the southern part of the region as shown in Figures 3d–f. The upper part of the ridge can be regarded as an earthquake prone zone. The spatial distribution of earthquake energy along the ridge reveals a prominent large weighted sum of earthquake energy. Thus, this ridge can also be categorized as being an earthquake zone that can generate tsunamis.

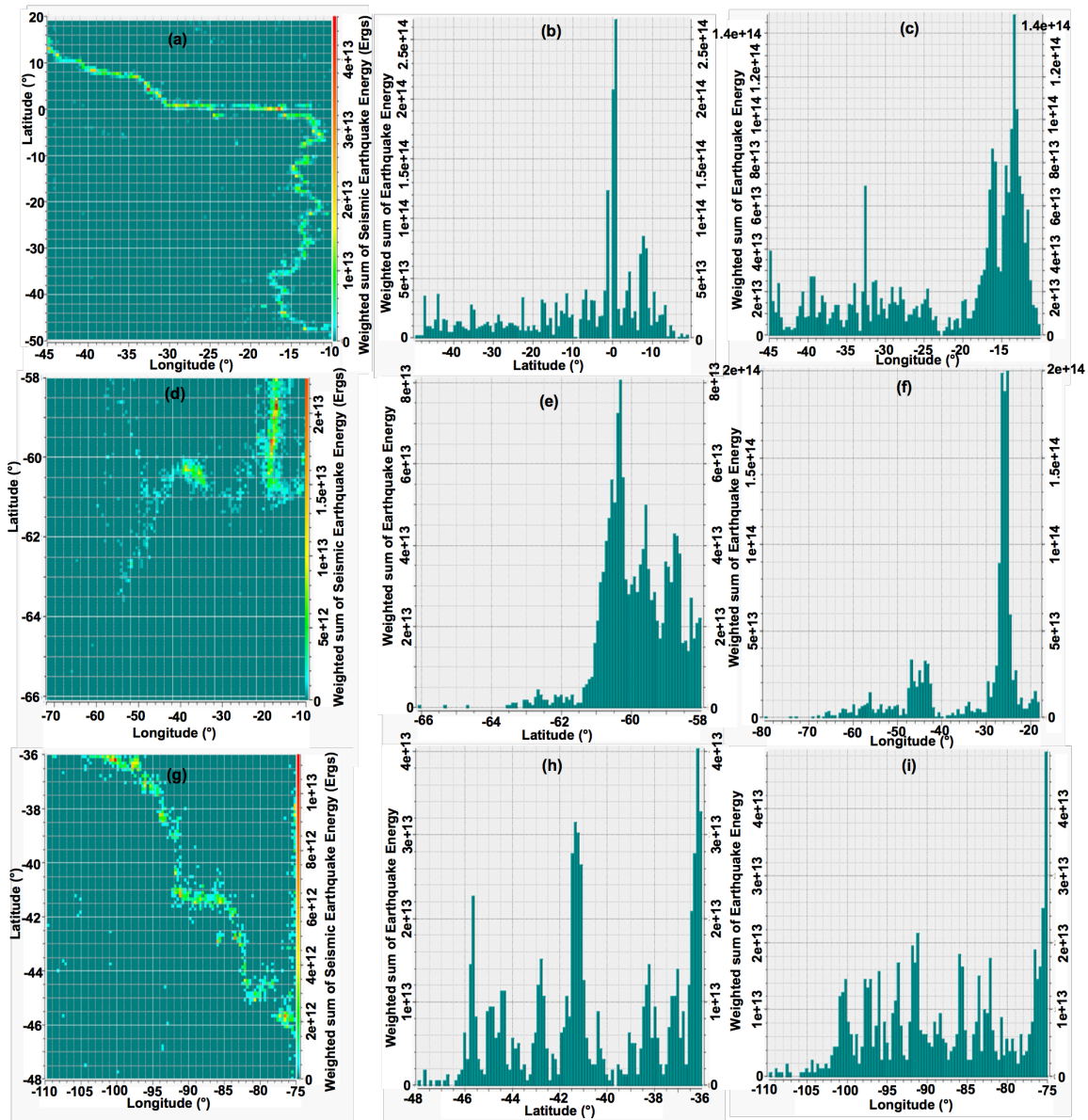


Figure 3: Spatial distribution maps of weighted sum of earthquake energy released. (a) Mid-Atlantic Ridge. (b) Latitudinal coordinate epicenter in Mid Atlantic Ridge. (c) Longitudinal coordinate epicenter in Mid Atlantic Ridge. (d) Pacific Ridge. (e) Latitudinal coordinate epicenter in Pacific Ridge. (f) Longitudinal coordinate epicenter in Pacific Ridge. (g) Chile Ridge. (h) Latitudinal coordinate epicenter in Chile Ridge. (i) Longitudinal coordinate epicenter in Chile Ridge.

The spatial distribution of earthquake energy in the Chile Ridge, as illustrated in Figure 3g, shows that the earthquake energy is evenly distributed across the entire length. The study of both latitudinal and longitudinal coordinates of earthquake epicenters indicates that earthquake energy released on the ridge is evenly distributed (Figures 3h and i). Large earthquake energy seems to be present in the entire region. Therefore, the earthquake energy distribution along the Chile Ridge, indicates that it is a seismically very active earthquake zone that can generate destructive tsunamis.

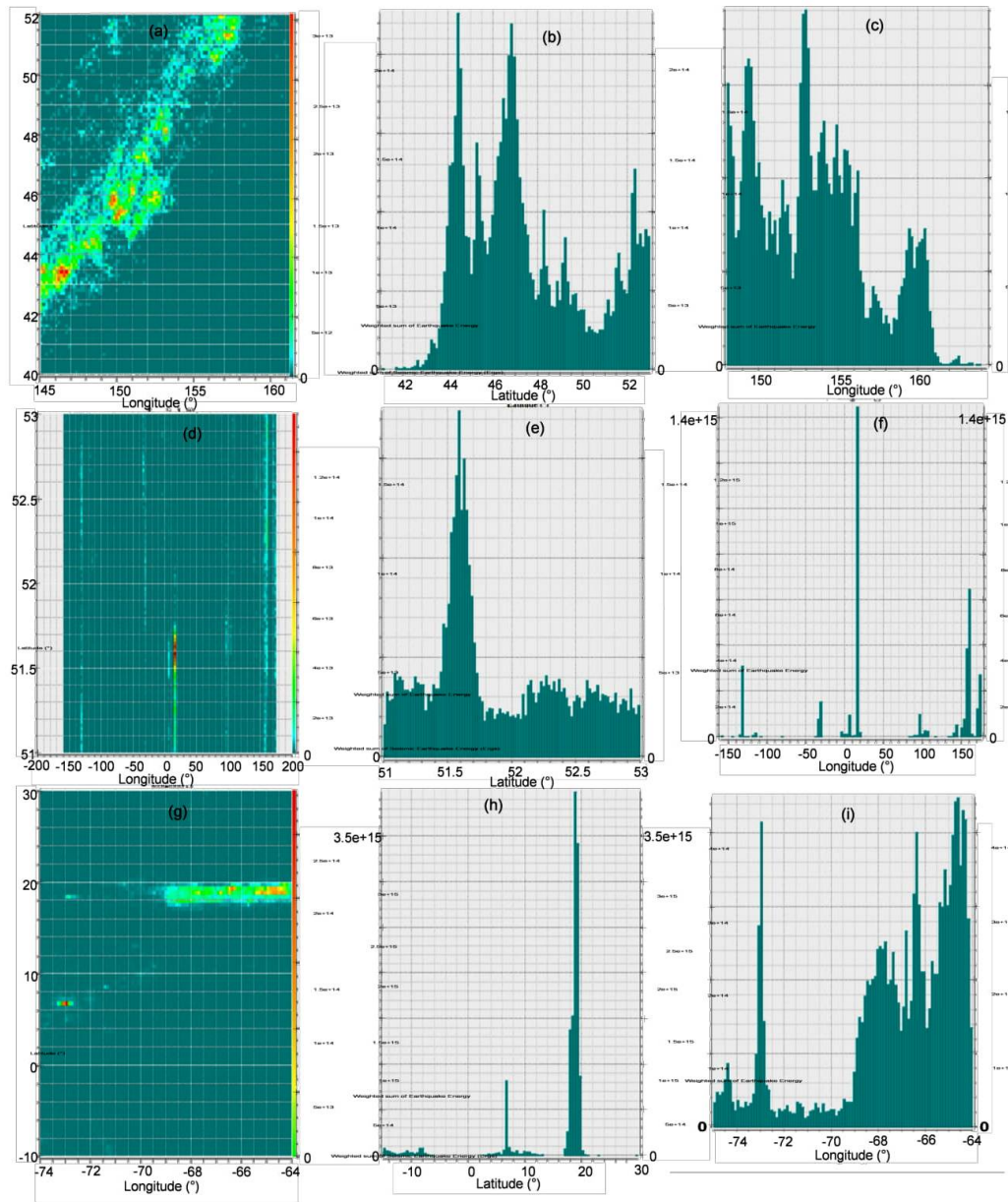


Figure 4: Spatial distribution maps of weighted sum of earthquake energy released. (a) Japan Trench. (b) Latitudinal coordinate epicenter in Japan Trench. (c) Longitudinal coordinate epicenter in Japan Trench. (d) Aleutian Trench. (e) Latitudinal coordinate epicenter in Aleutian Trench. (f) Longitudinal coordinate epicenter in Aleutian Trench. (g) Peru-Chile Trench. (h) Latitudinal coordinate epicenter in Peru-Chile Trench. (i) Longitudinal coordinate epicenter in Peru-Chile Trench.

### 3.2 Analysis of the Weighted sum of Earthquake Energy along Oceanic Trenches

Figure 4a shows the 2-dimensional image of the weighted sum of earthquake energy along the Japan Trench. The earthquake energy released in this zone is heavily distributed in the northwestern and southwestern regions of the trench, but sparsely distributed in other parts of the trench. Figures 4b and 4c also reveal the image of the energy distribution along the coordinates of the epicenter that corroborates the 2-dimensional image of Figure 4a. Heavy distribution of energy along the Japan Trench indicates large accumulation of stress along this zone. The consequential effect of this can generate tsunamigenic earthquakes within the oceanic floor.

The Aleutian Trench cannot be regarded as tsunamigenic zone based on the fact that the spatial distribution of the weighted sum of earthquake energy in this subduction zone is sparsely concentrated in all the regions of the trench (Figure 4d). Large earthquake energy is seldom released in this trench. In the latitudinal and longitudinal coordinates, only minute portions of the trench experience large earthquake energy as shown in Figures 4e and 4f. The weighted sum of this energy can be regarded as 'negligible' based on its spatial distribution. This implies that this trench can be regarded as a fairly stable region with low seismicity.

Figure 4g, indicates that the earthquake energy distribution along the Peru-Chile Trench only dominates its northeastern part and sparsely the other parts of the trench. Figures 4h and 4i illustrate that the weighted sum of energy released in the trench is very large in the eastern and northern part. This analysis implies that the Peru-Chile Trench can be regarded as tsunamigenic earthquake zone.

### 3.3 Interpretation of Gutenberg – Richter relation constants in oceanic ridges and Trenches

The frequency magnitude distribution showing “a” and “b” values for the Mid-Atlantic, the Pacific and the Chile Ridges as well as for the Japan, the Peru-Chile, and the Aleutian Trenches (Figures 5a–f) show the Gutenberg – Richter relation parameters (a and b values) in the oceanic ridges and trenches. The “a” and “b” are real constants with values which vary in space and time. Parameter “a” characterizes the general level of seismicity in a given area during the study period - the higher the *a* value, the higher the seismicity. The parameter “b” commonly called the *b*-value has been widely used in the study of seismicity, tectonics, seismic risk estimation and earthquakes prediction. The *b*-value indicates the tectonic character of a region and assumed to depend on the accumulated stress in that region (Nuannin, 2006). Schorlemmer *et al.* (2004) described *b*-value as a stress meter, depending inversely on the differential stress. Therefore, the lower the “b” value, the higher is the tectonic stress in the region (Adagunodo et al. 2018a; b).



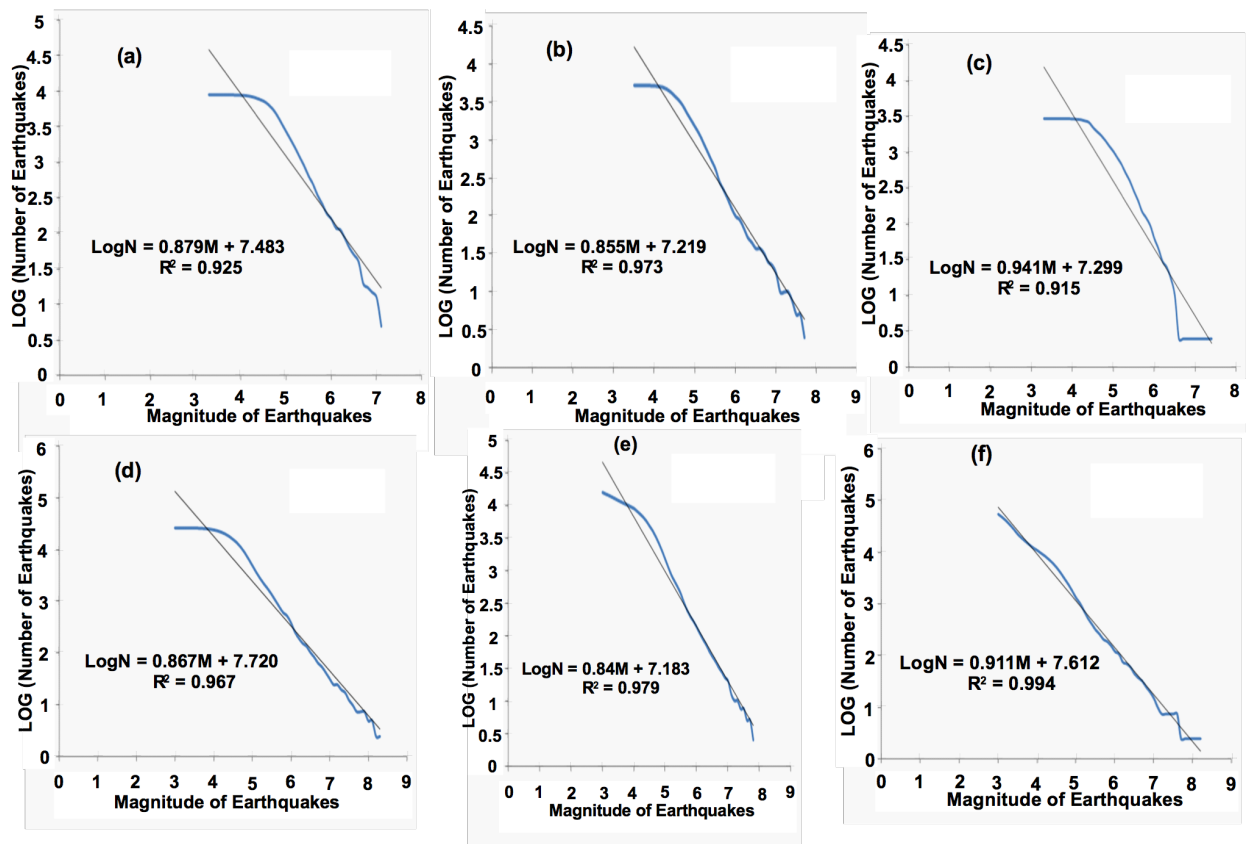


Figure 5: Maps of FMD of earthquakes in the study locations. (a) Mid-Atlantic Ridge (1978-2017). (b) Pacific Ridge (1978-2017). (c) Chile Ridge (1978-2017). (d) Japan Trench (1978-2017). (e) Aleutian Trench (1978-2017). (f) Peru-Chile Trench (1978-2017).

### 3.4 Interpretation of Gutenberg – Richter “a” value

In the ridges and trenches, the a-value that was obtained is far greater than one. This signifies that there is an increase in the occurrences earthquakes in ridges and trenches. The earthquakes recorded in Mid-Atlantic Ridge outnumbered those recorded in along the Pacific and Chile Ridges respectively. This implies that numerous significant tsunamigenic earthquakes had been occurring in all these ridges but more predominantly in the Mid–Atlantic Ridge. Furthermore, the earthquakes recorded along the Japan Trench outnumbered those recorded along the Aleutian and Peru-Chile Trenches, respectively. This implies that numerous significant tsunamigenic earthquakes had been occurring along all these trenches as well, but more prevalent in the Japan Trench. In comparison, the earthquake events in Trenches outnumbered that of Ridges. Thus, trenches are more prone to earthquakes than the ridges. Computation of a-values from the six study locations is presented in Table 1.

### 3.5 Interpretation of Gutenberg –Richter “b” value

The low  $b$ -values ( $b \ll 1$ ) obtained in the ridges and trenches reveal that the rate of tectonic stress accumulation is very high, an indication of increase in the rate of divergence and convergence of lithospheric plates, along the ridges and trenches respectively. The high rate of divergence of tectonic plates in the ridges and convergence in the trenches implies that the lithospheric plates are becoming more unstable and tectonic stress accumulation is increasing in both the ridges and trenches. Therefore, these regions can be regarded as seismogenic zones. Computation of  $b$ -values from the investigated ridges and trenches are shown in Table 1.

Table 1: Distribution of  $a$ - and  $b$ -values in the oceanic ridges and trenches (1978-2017)

Location	$a$ -value	$b$ -value
Mid-Atlantic Ridge	7.483	0.879
Pacific Ridge	7.219	0.855
Chile Ridge	7.299	0.941
Japan Trench	7.720	0.867
Aleutian Trench	7.183	0.840
Peru-Chile Trench	7.612	0.911

### 3.6 Temporal variation of $b$ -value along the ridges and trenches

Temporal variation of “ $b$ ” values along the oceanic ridges and trenches as shown in Figures 6a and b revealed that earthquakes of large magnitudes occurred in intervals of low  $b$ -values. A significant drop in  $b$ -value indicates an increase in the stress level. The  $b$ -value mapping is therefore a useful tool to display variation of stress accumulation over large areas (Awoyemi et al., 2017). In Figures 6a and b, a V-shape curve is experienced as the  $b$ -values drop with respect to time, which corresponds to large earthquakes ( $\geq M6$ ). A rapid decrease in  $b$ -value with time was observed prior to the occurrence of large earthquakes, and rapid increase in  $b$ -value was also observed after the occurrence of large earthquakes. Therefore, this anomalous variation of  $b$ -value with time may be considered as a precursor for earthquake prediction in the ridges and trenches. In Figure 6a, the low temporal  $b$ -values are associated with earthquakes along the Mid – Atlantic, the Pacific and the Chile Ridges. This is an indication of increase in tectonic stress level in the oceanic ridges. The lowest “ $b$ ” value was observed for the Mid – Atlantic Ridge. The  $b$ -value associated with the earthquakes the Pacific Ridge is lower than that of the Chile Ridge. Based on this, the Mid – Atlantic Ridge can be regarded as the most tsunamigenic earthquake zone of all three ridges. In the same vein, Figure 6b revealed low temporal  $b$ -values in the investigated trenches. The estimations of  $b$ -value from the three investigated trenches are in the order: Japan Trench < Peru-Chile Trench < Aleutian Trench. Therefore, Japan Trench can be regarded as the most tsunamigenic earthquake zone of all these trenches.

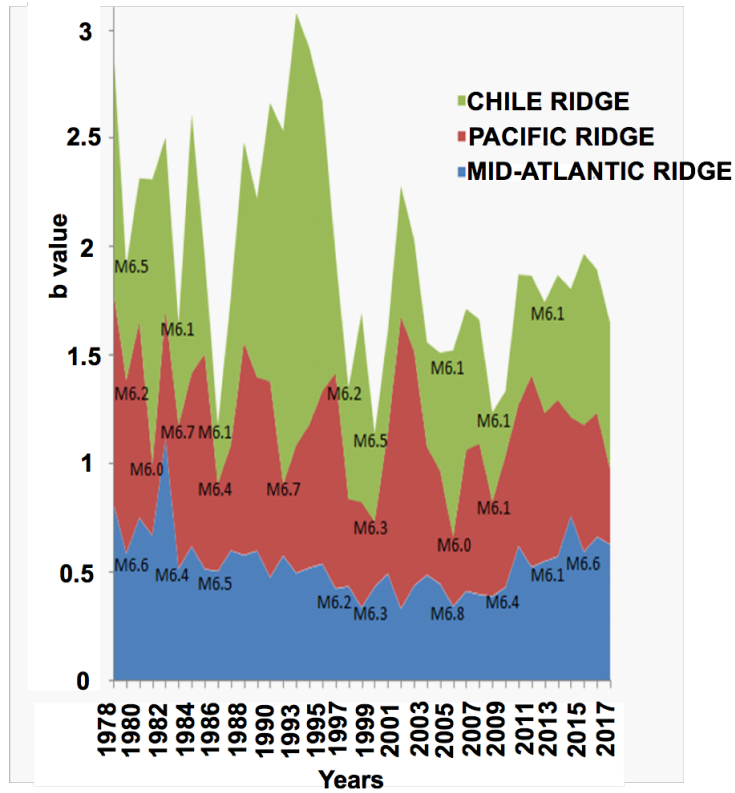


Figure 6a: Temporal variation of b-value in Oceanic Ridges

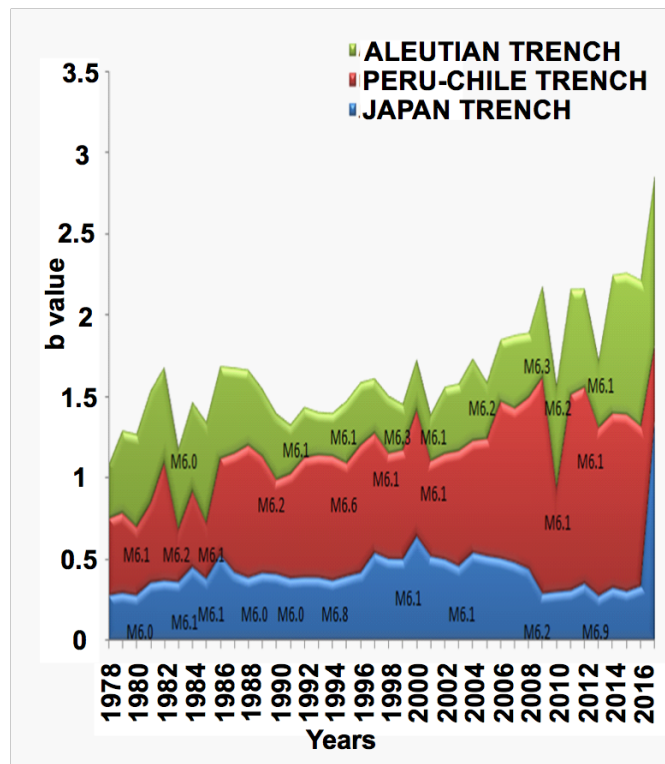


Figure 6b: Temporal variation of b-value in Oceanic Trenches

#### 4.0 CONCLUSIONS

The cluster of large earthquake energy in the northeastern part of the Mid-Atlantic ridge and the northern part of the Pacific Ridge is an indication that the region has high potential for the generation of tsunamis. The spatial distribution of earthquake energy in the Chile Ridge indicates that the earthquake energy released is evenly distributed across the ridge. However, the Chile Ridge can also be regarded as being a region of high tsunamicity. The earthquake energy released in the Japan Trench is heavily distributed in its northwestern and southwestern of the trench and sparsely distributed along the other parts of the trench. The earthquake energy distribution along the Peru-Chile Trench appears to be only concentrated along the northeastern part of the trench and sparsely distributed along its other parts of the trench. This implies that earthquakes along the Japan and Peru-Chile trenches can be regarded as having a high potential to generate tsunamis with greater frequency, while tsunamigenic earthquakes along the Aleutian Trench are less frequent - cannot be regarded as such based on the fact that the spatial distribution of the weighted sum of earthquake energy in this subduction zone is sparsely distributed in all the regions of the trench. Only the Aleutian Trench can be regarded as fairly stable trench (with low seismicity) of all the trenches, because large earthquake energy is only experienced in minute portions of the trench.

The b-values associated with the earthquake in the oceanic Ridges and Trenches were also investigated in order to identify the tsunamigenic zones in the study locations. Low temporal b-values are associated with earthquakes in Mid-Atlantic Ridge, Pacific Ridge and Chile Ridge, an indication of increase in tectonic stress level in the oceanic ridges. Of all the oceanic ridges, The Mid-Atlantic Ridge depicted the least b-value, while the Chile Ridge depicted the highest b-value. Based on this, the Mid-Atlantic Ridge can be regarded as the most tsunamigenic earthquake zone of all the ridges. From the oceanic trenches the Japan Trench depicted the least b-value, while the Aleutian Trench depicted the highest b-value. Therefore, the Japan Trench can be regarded as the most tsunamigenic earthquake zone of all the trenches.

## ACKNOWLEDGMENT

We acknowledge the publication support received from Covenant University, Nigeria.

## REFERENCES

**Abe, K.** (1981). *Physical size of tsunamigenic earthquakes of the northwestern Pacific*. *Phys. Earth Planet. Inter.* 27 (3): 194–205.

**Adagunodo T.A. and Sunmonu L.A.** (2015). Earthquake: a Terrifying of all Natural Phenomena. *Journal of Advances in Biological and Basic Research*. 01(1): 4–11.

**Adagunodo T.A., Oyeyemi K.D., Hammed O.S., Bansal A.R., Omidiora J.O., Pararas-Carayannis G.** (2018a). Seismicity Anomalies of M 5.0 + Earthquakes in Chile during 1965 – 2015. *Science of Tsunami Hazards*, 37(2): 130 – 156. <http://www.tsunamisociety.org/STHVol37N2Y2018.pdf>.

**Adagunodo T.A., Lüning S., Adeleke A.M., Omidiora J.O., Aizebeokhai A.P., Oyeyemi K.D., Hammed O.S.** (2018b). Evaluation of  $0 \leq M \leq 8$  Earthquake Data Sets in African-Asian Region during 1966 – 2015. *Data in Brief*, 17C: 588 – 603. <https://doi.org/10.1016/j.dib.2018.01.049>.

**Amiri G.G., Razeghi H.R., RazavianAmreiS.A., Aalae H., Rasouli S.M.** (2008). Seismic Hazard Assessment of Shiraz, Iran. *Journal of Applied Sciences*. 8:38-48.

**Ammon, C.J.; Kanamori H.; Lay T.; Velasco A.A.** (2006). [The 17 July 2006 Java tsunami earthquake \(PDF\)](#). 33. *American Geophysical Union: L24308*. [Bibcode:2006GeoRL..3324308A](#). [doi:10.1029/2006GL028005](#). Retrieved 23 July 2011.

**Awoyemi M.O., Hammed O.S., Shode O.H., Olurin O.T., Igboama W.N., Fatoba J.O.** (2017). Investigation of b-value variations in the African and parts of Eurasian plates. *Journal of Tsunami Society International*, 36(2): 86 – 99.

**Awoyera P. O., Ogundeji J. and Aderonmu P.A.** (2016). *Simulated Combined Earthquake and Dead Load Lateral Resistance Building Systems using Nigeria Seismic Data*. *Journal of Materials and Environmental Science*, 7 (3): 781-789. ISSN 885-894.

**Awoyera P.O., Ngene B.U., Adeyemi G.A., Aderonmu P.A.** (2017). *Mitigating Ground Shaking Construction Activities in Coastal Cities of Nigeria: An Earthquake Preventive Measure*. In: *Earthquakes: Monitoring Technology, Disaster Management and Impact Assessment*. Nova Science Publishers, Inc.. ISBN 978-1536103427.

**Bryant, E.** (2008). *5-Earthquake-generated tsunami*. [Tsunami: the underrated hazard \(2 ed.\)](#). Springer: pp. 129–138. [ISBN 978-3-540-74273-9](#). Retrieved 19 July 2011.

**Damanik, R., Andriansyah, Putra, H. K., Zen, M. T.** (2010). Variations of b-values in the Indian Ocean-Australian Plate Subduction in South Java Sea. Proceedings of the Bali 2010 International Geosciences Conference and Exposition, Bali, Indonesia: 19 – 22

**Ghosh A.** (2007) Earthquake frequency-magnitude distribution and interface locking at the middle America subduction zone near Nicoya Peninsula Costa Rica Georgia institute of technology. <http://smartech.gatech.edu/handle/1853/16288>

**Hammed O.S., Popoola O.I., Adetoyinbo A.A., Awoyemi M.O., Adagunodo T.A., Olubosede O., Bello A.K.** (2018). Peak Particle Velocity Data Acquisition for Monitoring Blast Induced Earthquakes in Quarry Sites. Data in Brief, 19: 398 – 408. <https://doi.org/10.1016/j.dib.2018.04.103>.

**Hammed O.S., Popoola O.I., Adetoyinbo A.A., Awoyemi M.O., Badmus G.O., Ohwo O.B.** (2013). Focal depth, magnitude, and frequency distribution of earthquakes along Oceanic Trenches. Earthquake Science, 26: 75 – 82.

**Ishibashi, K.** (2004). [Status of historical seismology in Japan](#). *Annals of Geophysics*. 47 (2/3): 339–368. Retrieved 22 November 2009.

**Kanamori, H.** (1972). [Mechanism of tsunami earthquakes](#). *Physics of the Earth and Planetary Interiors*. 6: 346–359. [Bibcode:1972PEPI...6..346K](#). [doi: 10.1016/0031-9201\(72\)90058-1](#). Retrieved 19 July 2011.

**Kanamori, Hiroo; Kikuchi, Masayuki** (1993). [The 1992 Nicaragua earthquake: a slow tsunami earthquake associated with subducted sediments](#). *Nature*. 361 (361): 714–716. [Bibcode:1993Natur.361..714K](#). [doi:10.1038/361714a0](#).

**Pararas-Carayannis, G.** (1967). Source Mechanism Study of the Alaska Earthquake and Tsunami of 27 March 1964, The Water Waves. Pacific Science. Vol. XXI, No. 3, July 1967.

**Pararas-Carayannis, G.** (2007). [The Earthquake and Tsunami of 2 September 1992 in Nicaragua](#). [Archived from the original on 17 May 2008](#). Retrieved 2008-06-09.

**Pararas-Carayannis, G.** (2011). The earthquake and tsunami of July 21, 365 AD in the Eastern Mediterranean Sea - Review of impact on the ancient world - assessment of recurrence and future impact. 30 (4): 286.

**Polet, J. & Kanamori H.** (2000). [Shallow subduction zone earthquakes and their tsunamigenic potential](#). *Geophysical Journal International. Royal Astronomical Society*. 142: 684–702. [Bibcode: 2000GeoJI.142..684P](#). [doi:10.1046/j.1365-246X.2000.00205.x](#). Retrieved 23 July 2011.

**Schorlemmer, D., S. Wiemer, and M. Wyss** 2004. Earthquake Statistics at Parkfield I: Stationarity of b-values. Journal of Geophysical Research 109

**Tanioka, Y.; Seno T. (2001).** [Sediment effect on tsunami generation of the 1896 Sanriku tsunami earthquake.](#) *Geophysical Research Letters*. 28 (17): 3389 - 3392.

**Tsuboi, S. (2000).** [Application of  \$M\_{wp}\$  to tsunami earthquake.](#) *Geophysical Research Letters*. *American Geophysical Union*. 27 (19). [Bibcode:2000GeoRL..27.3105T](#). [doi:10.1029/2000GL011735](#). Retrieved 19 July 2011.